

# A Falsifiable Dark Energy Model: Holographic Dark Information Energy

Michael Paul Gough

School of Engineering & Design, University of Sussex, Brighton, BN1 9QT, United Kingdom  
E-Mail: m.p.gough@sussex.ac.uk

**Abstract:** Several models have been proposed to explain the dark energy that is causing universe expansion to accelerate. Here the acceleration predicted by the Holographic Dark Information Energy (HDIE) model is compared to the acceleration that would be produced by a cosmological constant. While identical to a cosmological constant at low redshifts,  $z < 1$ , the HDIE model results in smaller Hubble parameter values at higher redshifts,  $z > 1$ , reaching a maximum difference of  $2.6 \pm 0.5\%$  around  $z \sim 1.7$ . The next generation of dark energy measurements, both those scheduled to be made in space (ESA's Euclid and NASA's WFIRST missions) and those to be made on the ground (BigBOSS, LSST and Dark Energy Survey), should be capable of determining whether such a difference signature exists or not. The HDIE model is therefore falsifiable.

**Keywords:** Landauer's principle, Holographic principle, Dark energy, Cosmology

**PACS Codes:** 89.70.Cf, 95.36.+x, 04.70.Dy, 98.80.Es

## 1. Introduction

The expansion of the universe is accelerating, driven by a dark energy that presently accounts for around three quarters of the total energy of the universe. This conclusion, initially obtained using type 1A supernova as reference sources [1, 2], is supported by more recent supernova measurements [3] and now confirmed by a number of independent measurements [4-7]. The large dark energy component is evident in gravitational weak lensing [4], in the projected scale of baryon acoustic oscillations [5], in the Cosmic Microwave Background radiation anisotropies [6], as well as in the growth rate of large scale structure, or clustering power spectrum of galaxies [7] (see reviews [8, 9]).

The many explanations proposed to explain dark energy include: Einstein's cosmological constant; some form of quintessence field; and a wide range of 'alternative models' [8, 9]. Two properties are required for a dark energy model to fit the observations. Firstly, at least for the recent period, redshifts  $z < 1$ , the model must provide a near constant energy density, equivalent to a total dark energy that increases as  $\sim a^3$ , where  $a$  is the universe scale size (size relative to today,  $a=1$ ). This is equivalent to an equation of state value  $w \sim -1$ , since energy densities vary as  $a^{-3(1+w)}$ . Secondly, the model must also be capable of quantitatively accounting for that dark energy density value, a high value, three times the energy density equivalence of the universe's present total mass density. Ideally we wish to find a model that satisfies these two requirements without recourse to exotic or unproven physics.

Foremost amongst likely explanations is the cosmological constant, or vacuum energy, that satisfies the first of our two requirements, by definition exhibiting a constant energy density, equivalent to the specific equation of state value  $w = -1$ . In contrast, quintessence is a scalar field with a dynamic equation of state that varies over space and time. Experimental measurements at low redshifts,  $z < 1$ , limit the dark energy equation of state to lie within the narrow range  $w = -0.94 \pm 0.09$  [10] and thus generally favour the cosmological constant explanation. Accurate measurements of dark energy at higher redshifts,  $z > 1$ , await the next generation of measurements. Unfortunately, satisfying the second of our requirements is more difficult as there are only two possible energy density values expected for a cosmological constant from quantum field theories [11]. The cosmological constant should either have a preferred value some 120 orders of magnitude higher than that required - a value impossible to reconcile with our universe, or it has the value zero. Then a different dark energy explanation would, if correct, enable the cosmological constant to take this second natural value: zero.

The model considered in this paper is the Holographic Dark Information Energy, HDIE, model [12]. Although HDIE belongs to the broad category of ‘alternative models’, HDIE easily satisfies our two required dark energy properties at low redshifts mainly by applying proven physics (see discussion at end of section 2). Nevertheless, HDIE is only one of the many dark energy models proposed to date and science progress requires that we eliminate all but one. With that elimination in mind, the emphasis here is on the HDIE model’s predicted signature that differentiates HDIE from other models/theories. The HDIE model is shown below to be *falsifiable* [13] since a failure to observe its predicted specific signature would clearly exclude this model. Note that there is an inherent lack of symmetry in falsification arguments. Although a positive observation of this signature would exclude a cosmological constant, it would not necessarily exclude all other models. For example, some form of quintessence field might produce a similar signature to that described below for HDIE, but then that model would also need to be equally capable of explaining the specific form of that observed signature.

In general, other models concentrate on providing a cosmological constant-like behaviour [7][8], rather than quantifying any measurable difference, such as provided below for HDIE.

## 2. The HDIE model

The HDIE model has been described in detail before [12] and only relevant features are recounted here. Essentially, HDIE combines Landauer’s principle [14] with the Holographic principle [15].

Landauer’s principle[14][16-18] states that any ‘erasure’ of information, or reduction of information bearing degrees of freedom, requires a minimum of  $k_B T \ln 2$  of heat per erased bit to be dissipated into the surrounding environment. This dissipated heat increases the thermodynamic entropy of the surrounding environment to compensate for the loss of degrees of freedom and comply with the 2<sup>nd</sup> law. Information is not destroyed as the ‘erased’ information is now effectively contained in the extra degrees of freedom created in the surrounding environment.

Heat dissipation from information erasure is comparatively weak and usually insignificant in our normal day to day experience. For example, world-wide, man-kind has now accumulated some  $10^{22}$  bits of stored digital data and we have the technological capacity to process a total of around  $3 \times 10^{19}$

instructions per second in general-purpose computers [19]. We can assume that the main information erasure that occurs during the process of computing is caused by the overwriting the processor's instruction register when each new instruction is read from memory. In this way man-kind erases some  $10^{21}$  bits each second. At room temperature this rate of information erasure will generate a world-wide total of only 3W! This is insignificant,  $\sim 10^{-11}$  of the total heat dissipation (ohmic and inductive heating, etc) of the world's  $\sim 10^9$  computer systems that each dissipate  $\sim 10^2$ W. Similarly, erasing the  $10^{22}$  bit sum total of all man made stored digital data would only generate a world-wide total of just 3J.

Despite this low bit equivalent energy, the information-to-energy conversion process has been demonstrated experimentally using Brownian particles under feedback control [20] and by a one-bit memory consisting of a single colloidal particle trapped in a modulated double-well potential [21]. Moreover, Landauer's heat dissipation from information erasure is still considered the best way to reconcile Maxwell's Demon with the second law of thermodynamics [18 & 22, and references therein].

Landauer's principle provides the information energy equivalence, similar to the  $mc^2$  energy equivalence for mass. When the same degrees of freedom are considered information entropy and thermodynamic entropy are identical. Then every component of the universe has an information equivalent energy of  $Nk_B T \ln 2$  that depends on the quantity of information (or entropy),  $N$  bits, associated with the component and on the component's temperature,  $T$ .

The Holographic principle [15] states that the amount of information in any region,  $N$ , scales with that region's bounding area. The Holographic Principle lead directly from the discovery that the maximum entropy of a black hole is set by its surface area [23] but the principle is considered to have universal validity [24], i.e. not just limited to the maximum entropy limit of black holes.

The information energy contributions of the various components of the universe have been compared before by comparing estimates of  $N$  and  $T$  for each [12]. It was found that the greatest contribution to the information energy of the universe is made by stellar heated gas and dust. Black holes could make the next strongest contribution at a few percent of that level (see Table 1 of [12]) but it is doubtful whether the information within a black hole, and therefore its information energy, has any effect on the universe because of the 'no hair theorem' [25]. While a black hole may exert a significant gravitational force on local objects, the only information that the universe has about it is limited to just three parameters: mass; charge; and angular momentum. From the universe's information point of view a black hole is no more than just another single fundamental particle, albeit a massive one!

Since the information energy,  $Nk_B T \ln 2$ , of the universe is primarily determined by stellar heated gas and dust, the appropriate temperature,  $T$ , will be the average temperature of baryons in the universe. Figure 1 upper panel plots the average baryon temperature,  $T$ , data and the fraction of baryons in stars,  $f$ . The data points (various symbols) shown are re-plotted from [12], where all data source references can be found.

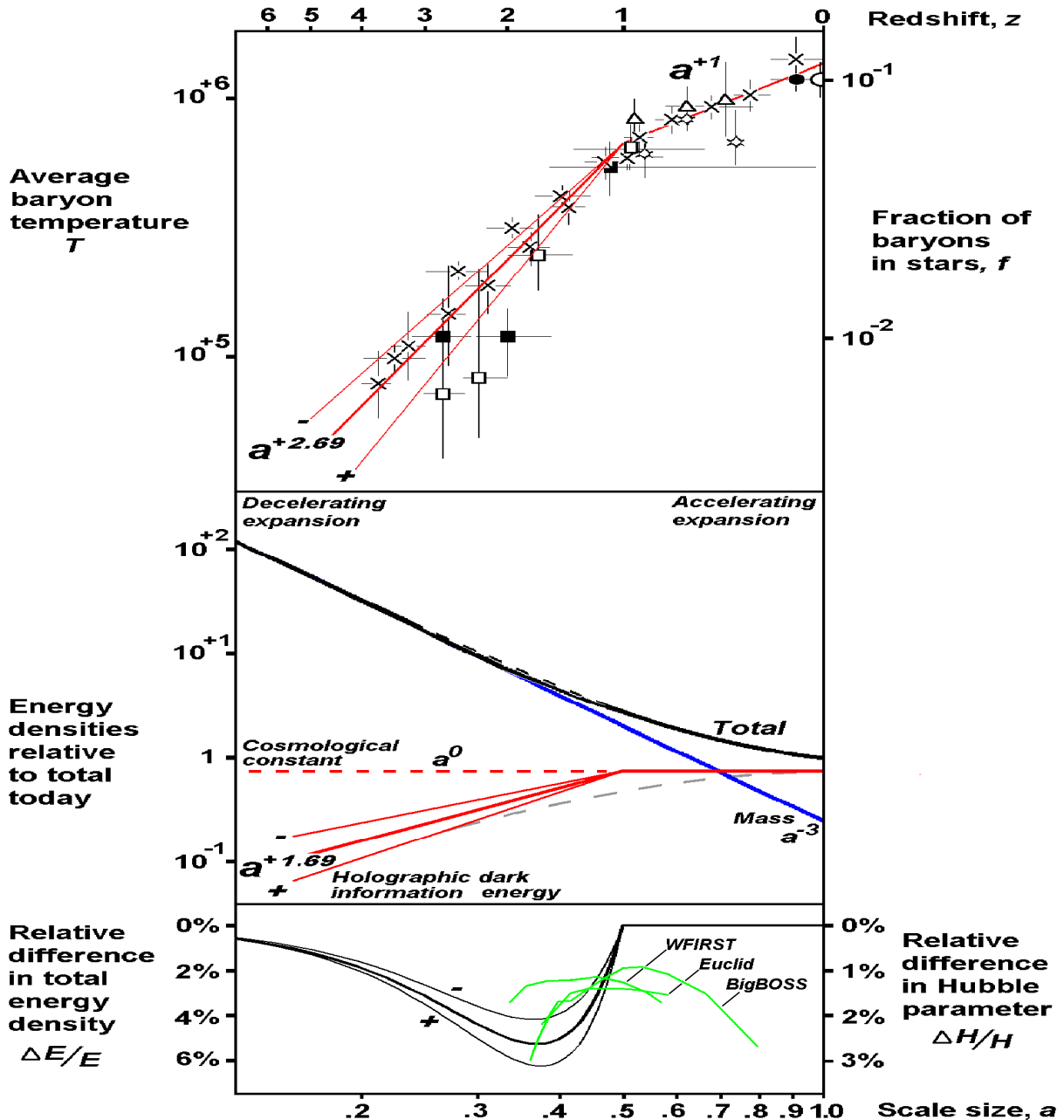


**Figure 1.** Plotted against log of universe scale size,  $a$ , are three panels:

**Upper Panel:** Log plot of measured average baryon temperature,  $T$ , and the fraction of all baryons in stars,  $f$  (various symbols- see text). Red lines- fits to data points of  $a^{+0.98 \pm 0.17}$  for  $z < 1$ , and  $a^{+2.69 \pm 0.43}$  for  $z > 1$ , with limiting gradients for  $z > 1$  included as +, - .

**Middle Panel:** Log plot of energy density contributions: red continuous lines, HDIE energy densities corresponding to the red line fits in the upper panel; dashed red line, cosmological constant; blue line, mass; solid black line, total for HDIE case; dashed black line, total for the case of a cosmological constant; grey dashed curve, to illustrate problem of two parameter dynamic  $w$  model approximation.

**Lower Panel:** Linear plot of relative differences in total energy, and in Hubble parameter, between the HDIE model and a cosmological constant. The resolving thresholds of three next generation space and ground based measurements are shown for comparison in green.

The average temperature of baryons today is  $T \sim 2 \times 10^6$  k, which together with the estimate of  $N \sim 10^{86}$  from surveys (Table 1 of [12]) provides a quantitative estimate of the present HDIE energy value within an order of magnitude of the observed dark energy. We find that, despite the very low bit equivalent energy, information energy still manages to provide a significant contribution on cosmic scales, primarily because the universe's mass has remained constant while both the quantity of information (entropy),  $N$ , and the average baryon temperature,  $T$ , have increased continuously. Furthermore, data points in Figure 1 upper panel for the redshift range  $z < 1$  exhibit a best fit temperature gradient of  $a^{+0.98 \pm 0.17}$ . Then, assuming the total bit number,  $N$ , scales as  $a^{+2}$  from the holographic principle, the total HDIE energy for  $z < 1$  scales as  $a^{+2.98 \pm 0.17}$ . Since universe volume increases as  $a^3$ , there is a nearly constant HDIE energy density at  $z < 1$  with the HDIE equation of state lying in the narrow range  $-0.94 > w_{HDIE} > -1.05$ .

HDIE easily satisfies our two principal requirements for a successful explanation of dark energy. For the redshifts  $z < 1$  the HDIE equation of state range is limited to a narrow range,  $-0.94 > w_{HDIE} > -1.05$ , which includes the specific expected value,  $w_{DE} = -1$ . Also the estimated HDIE dark energy density value is within an order of magnitude of that required to explain the present accelerating expansion. Note that the latter directly depends on our estimate of  $N$  for stellar heated gas and dust, only accurate to a couple of orders of magnitude.

Moreover, HDIE satisfies our two dark energy model requirements largely by using accepted physics. HDIE accounts for today's high dark energy value (requirement 2), by taking measurements of the present average baryon temperature (Figure 1, top panel, right-hand axis intercept), taking the best estimates of the information (entropy) associated with stellar gas and dust [12], and applying experimentally proven [20][21] Landauer's principle. HDIE accounts for the constant dark energy density  $z < 1$ , (requirement 1), by combining the measured average baryon temperature relation:  $T \propto a^{+1}$  at  $z < 1$  (figure 1, top panel), with the holographic principle relating information content to bounding area,  $N \propto a^{+2}$ . Now the Bekenstein-Hawking description [23] of a black hole, with entropy proportional to surface area, is widely accepted physics. But black holes exist at the maximum entropy holographic bound while the universe is some 30 orders of magnitude below the holographic bound. The holographic principle, naturally extending the  $N \propto a^{+2}$  relation to all objects including those well below their maximum entropy [24], remains an attractive but, as yet unproven, hypothesis. The holographic principle thus constitutes the only significant speculative aspect of the HDIE model.

### 3. HDIE model predictions for $z > 1$

Figure 1 upper plot shows that the temperature gradient was much steeper at redshifts  $z > 1$ , with a wider spread in measured data points and a best fit of  $a^{+2.69 \pm 0.43}$ . Clearly HDIE energy density was increasing in this earlier period up to the point around  $z \sim 1$  where HDIE leveled out at a near constant value that may account for all dark energy from that time onwards.

In the following analysis we therefore assume that the level HDIE energy density  $z < 1$  indeed accounts for all dark energy, and thus is located at a value three times the present mass energy density equivalent. Then Figure 1 middle plot shows the mass energy density falling as  $a^{-3}$  (blue line), the resulting HDIE energy density contribution with the above assumption (red lines), and a cosmological

constant for comparison (red dashed line). Because of the wide temperature data spread at  $z>1$  around the  $\sim a^{+2.69}$  middle gradient, we include the lower limit, best fit, and upper limit gradients of  $a^{+2.26}$ ,  $a^{+2.69}$ , and  $a^{+3.12}$  from Figure 1 upper panel with their corresponding HDIE energy density gradients (red lines) of  $a^{+1.26}$ ,  $a^{+1.69}$ , and  $a^{+2.12}$  respectively in Figure 1 middle panel. Information bit quantity,  $N$ , is again assumed to scale as  $a^2$  from the Holographic principle. Then the mean  $a^{+1.69}$  HDIE energy density variation corresponds to an equation of state  $w_{HDIE}=-1.56$  for  $z>1$ .

In Figure 1 middle panel we also compare the total energy density from HDIE + mass (black continuous line) with the total energy density of a cosmological constant + mass (black dashed line). At first sight the two total energy curves are very similar with little apparent difference because they are plotted on a multi-decade log-log plot.

Accordingly, in Figure 1 lower panel the relative difference in total energy density,  $\Delta E/E$ , between HDIE + mass and a cosmological constant + mass is shown on a linear-log plot for each of the three HDIE gradients. The three HDIE energy density gradients of  $a^{+1.26}$ ,  $a^{+1.69}$ , and  $a^{+2.12}$  in the middle panel then correspond to relative differences in total energy,  $\Delta E/E$ , in Figure 1 lower panel that peak at -4.2%, -5.2%, and -6.2% respectively at  $z\sim 1.7$ . Although there is a clear change in gradient around  $z\sim 1$  evident in the data points of Figure 1, upper panel, our fitting to gradients that change precisely at  $z=1$  may provide an overemphasized sharp transition in  $\Delta E/E$  at  $z=1$ . However, this transition should not significantly affect the size or the location of the predicted negative peak in  $\Delta E/E$  at  $z\sim 1.7$ . At earlier times,  $z>4$ , the higher mass density swamps any difference between HDIE and a cosmological constant. Later, as the mass density falls  $\Delta E/E$  begins to reflect the difference in the energy densities of the two dark energy components, peaking at  $z\sim 1.7$  as HDIE energy density rapidly increases as  $a^{+1.69\pm 0.43}$  towards  $z\sim 1$ , after which time there is no difference between models.

While the Hubble constant,  $H_0$ , is the fundamental relation between the recessional velocities of objects in the universe and their distance from us today,  $H_0$  is just the present value of the more general Hubble parameter,  $H$ . The Hubble parameter,  $H$ , varies with changes in universe expansion rate over time and is therefore a function of universe scale factor,  $a$ . Since total energy density,  $E$ , is proportional to  $H^2$ , (from the Friedmann equation, see for example [26]) these three curves then correspond to relative differences in Hubble parameter,  $\Delta H/H$ , that peak at -2.1%, -2.6% and -3.1% respectively. The HDIE model thus predicts that the Hubble parameter around  $z\sim 1.7$  should be  $2.6\pm 0.5\%$  less than that expected for a cosmological constant explanation for dark energy.

While this small difference in the Hubble parameter is not yet resolvable with today's instruments it falls within the observational capabilities of the next generation of space and ground based dark energy measurements. The future European Space Agency Euclid spacecraft [27], and the planned NASA WFIRST spacecraft [28] will both cover the redshift range  $0.7<z<2.0$ , while the ground based BigBOSS [29], LSST [30] and Dark Energy Survey [31] measurement campaigns will measure  $z<1.7$ ,  $z<5$  and  $z<2$ , respectively. These experiments utilise a combination of techniques: weak gravitational lensing to measure the growth of structure; supernova distances at low  $z$ ; and baryon acoustic oscillations at higher  $z$ . The resolving limits of three of these dark energy experiments are shown in Figure 1 lower panel (green lines) for comparison. The 2-3% difference in Hubble parameter around  $z\sim 1.7$  should be resolved by all three experiments. At the time of writing these next generation

measurement development timescales are: Dark Energy Survey starting a five year survey in 2012, BigBOSS first light 2016 with full science starting 2017; ESA Euclid launch 2019; LSST first light 2020 with full science starting 2022; and NASA WFIRST launch 2022.

Note that HDIE effectively provides a dynamic equation of state but, rather than a smooth variation, there are two distinct regimes:  $w_{HDIE}=-1$  for  $z<1$ ; and  $w_{HDIE}\sim-1.56$  for  $z>1$ . However, it is usual, for example in designing the above experiments, to characterise any dynamic equation of state,  $w(a)$ , by a smoothly varying two parameter model, typically given as :  $w(a)=w_p+w_a(1-a)$ , where  $w_p$  is the present value, the early value was  $w_p+w_a$ , and the mid-point transition occurs at  $a=0.5$ , or  $z=1$ . The experimental figure of merit is then determined by how small the error ellipse is in the  $w_p-w_a$  plane. For example, the ESA Euclid measurement accuracies equivalent to 1 sigma error are expected to be 0.02 in  $w_p$ , and 0.1 in  $w_a$  up to  $z\sim 2$  [27]. These accuracies are clearly sufficient to falsify HDIE where the nearest equivalent parameter values are  $w_p=-1$  and  $w_a=-0.56$ , as compared to the cosmological constant values of  $w_p=-1$  and  $w_a=0$ . Note that this form of  $w_p-w_a$  data analysis is not the ideal for HDIE because of the difference between such a smooth variation (grey dashed line in Figure 1 middle panel fitted to the high gradient limit for emphasis) and the more distinct transition expected at  $z\sim 1$  from HDIE. Rather than a single cluster of measurement data points on the  $w_p-w_a$  plane HDIE predicts two clusters: one at  $w_p=-1$  and  $w_a=0$  for  $z<1$ ; and one effectively at  $w_p=-1.56$  and  $w_a=0$  for  $z>1$ , since this later cluster is also independent of scale size,  $a$ , (i.e.  $w_a=0$ ) over that range  $z>1$ . Thus a determination of the Hubble parameter,  $H$ , as a function of scale factor,  $a$ , or redshift,  $z$ , is the more appropriate mode of data analysis to identify any signature of HDIE.

#### 4. Implications of HDIE

If the predicted HDIE model signature is indeed observed, and thus HDIE found to be the correct explanation for dark energy, there are some significant implications that follow for the cosmos.

The first concerns the reason why the temperature variation  $a^{+0.98 \pm 0.17}$  so closely follows  $a^{+1}$  since  $z\sim 1$  to provide the near constant HDIE energy density,  $-0.94 < w_{HDIE} < -1.05$ . If star formation had continued to proceed at the earlier, faster, rate, then it would have continued the steep  $a^{+2.69 \pm 0.43}$  average baryon temperature increase after  $z\sim 1$ . But this would have increased HDIE dark energy well above its present value, lead to much greater acceleration and greater expansion which, in turn, would have resulted in much less star formation. It would appear that since  $z\sim 1$  there has been a balance, or feedback, between expansion acceleration and star formation that has naturally maintained the star formation rate close to  $a^{+1}$  for a constant dark energy density. Note that the reduced rate of star and structure formation starting at  $z\sim 1$  was previously attributed to the onset of acceleration [32]. Thus HDIE provides a natural explanation for the reason why  $w_{DE} = -1$  since  $z\sim 1$ .

The second implication is that HDIE may lessen some of the cosmic coincidence problem. It is often thought that our existence just now in the era dominated by dark energy is an unlikely coincidence. However, HDIE dark energy density increased with increasing entropy and star formation while mass density decreased with increasing universe scale size. Provided it was reached before  $f\sim 1$ , there had to be a time when HDIE reached a level comparable to mass density to initiate acceleration. Similarly, the likelihood of our existence also increased as overall star formation increased, and thus was just as

likely to occur after star formation had reached that critical level. Perhaps a more interesting coincidence to consider is that the critical level was reached at  $f \sim 0.05$ , well before stellar formation could become saturated if  $f$  had approached closer to unity.

The third implication concerns how long the present period of accelerating expansion will last. Acceleration will continue provided that the overall universe equation of state,  $w < -1/3$  [9]. This threshold corresponds to HDIE energy density falling off as  $a^{-2}$ , and, assuming the total information,  $N$ , continues to follow the Holographic principle as  $a^{+2}$ , provides to a limiting average baryon temperature,  $T$ , variation of  $a^{-1}$ . Thus, acceleration due to HDIE will continue providing  $T$  does not fall off more steeply than  $a^{-1}$ . Computer simulations of future average baryon temperatures,  $T$ , up to  $a \sim 200$  [33], predict a leveling off of  $T$  since  $f$  is limited by definition to  $f < 1$ , with a slow eventual fall as star formation ceases, but falling less steeply than the threshold gradient of  $a^{-1}$ . Thus acceleration should continue, until at least the universe has increased in size by a factor of 200.

The fourth implication is that, should the predicted signature of HDIE be observed, it would provide very strong support for the holographic principle (see discussion at end of section 2). Attempts to directly verify the holographic principle by experiment are difficult and sometimes controversial [34].

While our main concern in this work has been to identify a measurable difference between HDIE and a cosmological constant, we conclude by highlighting an interesting similarity. Stellar heated gas and dust provides the main component of HDIE in our matter and dark energy dominated universe. The average baryon temperature today,  $T \sim 2 \times 10^6$ , corresponds to an average bit equivalent energy ( $k_B T \ln 2$ )  $\sim 120$  eV. Clearly this value would have been much lower if there had been no star formation. We can obtain a representative temperature for a hypothetical, similar mass density, universe without star formation, by assigning to it the temperature,  $T'$ , that a radiation dominated universe would need to have the same energy density:  $\rho c^2 = \sigma T'^4$ , where  $\rho$  is the universe mass density, and  $\sigma$  the radiation constant. Replacing the radiation constant by its definition in terms of fundamental constants, we obtain the equivalent bit energy,  $k_B T' \ln 2 = (15 \rho \hbar^3 c^5 / \pi^2)^{1/4} \ln 2$ . It has been previously noted [35][36] that this definition is identical to the characteristic energy of a cosmological constant (taking  $\ln 2 \sim 1$ , identical to equation 17:14 of [37]) and today has the value  $\sim 3 \times 10^{-3}$  eV, with  $T' \sim 35$ . Thus the, otherwise difficult to account for, low characteristic milli-eV energy associated with the cosmological constant [37] may be explained as an information bit equivalent energy.

## 5. Summary

In the redshift range  $z < 1$ , HDIE can account for all dark energy, both qualitatively and quantitatively. At higher redshifts, HDIE produces a clear signature, predicting that at  $z \sim 1.7$  the Hubble parameter will have a value  $2.6 \pm 0.5\%$  less than that expected for a cosmological constant. The HDIE model is falsifiable as the size and location of this predicted signature lies within the resolvable ranges of the next generation of dark energy measurements.

## References

1. Riess, A.G.; et al. Observational evidence from supernovae for an accelerating universe and a cosmological constant. *Astrophysical J.* **1998**, *116*, 1009-1038.

2. Perlmutter, S.; et al. Measurements of  $\Omega$  and  $\Lambda$  from 42 high-redshift supernovae, *Astrophysical J.*, **1999**, 517,565-586.
3. Riess, A.G.; et al. New Hubble Space Telescope Discoveries of Type 1a Supernovae at  $z \geq 1$ ; Narrowing Constraints on the Early Behaviour of Dark Energy, *Astrophysical J.*, **2007**, 659, 98-121.
4. Bacon, D.J.; Refregier, A.R.; Ellis, R.S. Detection of weak gravitational lensing by large-scale structure, *Mon. Not. R. Astron. Soc.* **2000**, 318, 625-640.
5. Beutler, F.; et al. The 6dF Galaxy Survey: Baryon Acoustic Oscillations and the Local Hubble Constant, *Mon. Not. R. Astron. Soc.* **2011**, 416, 3017-3032.
6. Sherwin, B.D.; et al. Evidence for dark energy from the cosmic microwave background alone using the Atacama Cosmology Telescope lensing measurements. *Phys. Rev. Lett.* **2011**, 107, 021302
7. Blake, C.; et al. The WiggleZ Dark Energy Survey: the growth rate of cosmic structure since  $z=0.9$ , *Mon. Not. R. Astron. Soc.* **2011**, 415, 2876-2891.
8. Carroll, S.M. Why is the universe accelerating? in *Carnegie Observatories Astrophysics Series, Vol2, Measuring and Modelling the universe*, ed. W.L.Freedmann, Cambridge University Press. 2003.
9. Frieman, J.A.; Turner, M.S.; Huterer, D. Dark Energy and the Accelerating Universe, *Ann. Rev. Astron. Astrophys.* **2008**, 46, 385-432.
10. Tegmark, M.; Eisenstein, D.J.; et al. Cosmological Constraints from the SDSS luminous red galaxies. *Phys. Rev. D* **2006**, 74, 123507, 34pages.
11. Weinberg, S. The Cosmological Constant Problem, *Rev. Mod. Phys.*, **1989**, 61, 1-23.
12. Gough, M.P. Holographic Dark Information Energy, *Entropy*, **2011**, 13, 924-935.
13. Popper, K. *The logic of scientific discovery*. Routledge ISBN 0-415-27844-9, London, UK, 1959.
14. Landauer, R. Irreversibility and heat generation in the computing process. *IBM J. Res. Dev.* **1961**, 3, 183-191.
15. 't Hooft, G. Obstacles on the way towards the quantization of space, time and matter- and possible solutions. *Stud. Hist. Phil. Mod. Phys.* **2001**, 32, 157-180.
16. Piechocinska, B. Information erasure. *Phys. Rev. A* **2000**, 61, 062314:1-062314:9.
17. Landauer, R. Dissipation and noise immunity in computation and communication. *Nature* **1988**, 335, 779-784.
18. Leff, H.S.; Rex, A.F.; Eds. Maxwell's Demon 2: Entropy, Classical and Quantum Information, Computing. IOP Publishing Ltd: London, UK, **2003**
19. Hilbert, M.; López, P. The World's Technological Capacity to Store, Communicate, and Compute Information. *Science* **2011**, 332, 60-65.
20. Toyabe, S.; Sagawa, T.; Ueda, M.; Muneyuki, E.; Sano, M. Experimental demonstration of information-to-energy conversion and validation of the generalized Jarzynski equality. *Nat. Physics* **2010**, 6, 988-992.
21. Be'rut, A.; Arakelyan, A; Petrosyan, A; Ciliberto, S; Dillenschneider, R; Lutz, E. Experimental verification of Landauer's principle linking information and thermodynamics. *Nature*, **2012**, Vol 483, 187-190.

22. Maruyama, K.; Nori, F. ; Vlatko Vedral, V. The physics of Maxwell's demon and information *Rev. Mod. Phys.* **2009**, *81*, No 1, 1-23.
23. Bekenstein, J.D. Black holes and entropy. *Phys. Rev. D* **1973**, *7*, 2333–2346
24. Susskind, L. The world as a hologram. *J. Math. Phys.* **1995**, *36*, 6377.
25. Ruffini, R.; Wheeler, J.A. Introducing the black hole. *Physics Today*, **1971**, *24*, 30-41.
26. Liddle, A.R. An introduction to Modern Cosmology (2<sup>nd</sup> edition), Wiley, Chichester, UK, **2003**.
27. Euclid Definition Study Report ESA/SRE[2011]12 July 2011  
<http://sci.esa.int/science-e/www/object/index.cfm?fobjectid=48983#> accessed Nov 8, **2011**.
28. NASA WFIRST Interim Report  
[http://wfirst.gsfc.nasa.gov/science/WFIRST\\_IDRM\\_Report\\_Final\\_signed\\_Rev2.pdf](http://wfirst.gsfc.nasa.gov/science/WFIRST_IDRM_Report_Final_signed_Rev2.pdf) accessed Nov 8, **2011**.
29. Schlegel, D.J.; et al. BigBOSS, The ground-based StageIV BAO Experiment, **2009**, ArXiv: 0904.0468v3.
30. Ivezić, Z.; et al. LSST: From science drivers to reference design and anticipated data products, **2011**, ArXiv: 0805.2366v2.
31. Dark Energy Survey proposal [www.darkenergysurvey.org/reports/proposal-standalone.pdf](http://www.darkenergysurvey.org/reports/proposal-standalone.pdf)  
Accessed Feb. 25, **2012**.
32. Guzzo, L., et al., A test of the nature of cosmic acceleration using galaxy redshift distortions, *Nature*, **2008**, *Vol 451*, 541-544.
33. Nagamine, K.; Loeb, A. Future evolution of the intergalactic medium in a universe dominated by a cosmological constant. *New Astron.* **2004**, *9*, 573–583.
34. Cho, A. Sparks Fly Over Shoestring Test Of 'Holographic Principle', *Science*, **2012**, *Vol 336*, 147-149.
35. Gough, M.P.; Carozzi, T.; Buckley, A.M. On the similarity of Information Energy to Dark Energy, **2006**, ArXiv: astro-ph/0603084.
36. Gough, M.P. Information Equation of State, *Entropy*, **2008**, *10*, 150-159.
37. Peebles, P.J.E. Principles of Physical Cosmology, Princeton University Press, **1993**.